DOI: 10.13009/EUCASS2019-454

Conceptual design of a Two-Stage-To-Orbit vehicle using SABRE engines

L. Brevault [a], M. Balesdent [a], R. Wuilbercq [a], N. Subra [a], S. Oriol [b], C. Bonnal [b], M. Dodds [c], N. Taylor [c] and R. Varvill [c]

[a]*DTIS, ONERA, Université Paris Saclay, F-91123 Palaiseau - France*
[b]*CNES, Launchers Directorate, Paris - France*
[c]*Reaction Engines Ltd., Culham - UK*

Abstract

The French Space Agency (Centre National d'Etudes Spatiales - CNES), the UK Space Agency (UKSA), Reaction Engines Limited (REL) and the French Aerospace Lab (Office National d'Etudes et de Recherches Aérospatiales - ONERA) share a common interest for future space launch architectures and technologies. Preliminary results of a joint study are presented in this paper with the main objective of assessing and quantifying the potential advantages and benefits of air-breathing propulsion technology developed by REL named SABRE (Synergetic Air-Breathing Rocket Engine) for future launch architectures. In that purpose, a conceptual study of two alternative Two-Stage-To-Orbit (TSTO) vehicles is carried out using the SABRE air-breathing rocket engine and a LOx/CH4 rocket engine (for the second stage) for the injection of a 15t payload into low Earth orbit. Different analyses are carried out using a coupled multidisciplinary process involving propulsion, aerodynamics, sizing and trajectory optimizations. Some key influential parameters and intricate behaviors are analyzed through sensitivity to the stage separation conditions. As a result, these analyses provide insight into technological requirements to achieve the target mission using these types of advanced propulsion technologies.

1. Introduction

The French Space Agency (CNES), the UK Space Agency (UKSA), Reaction Engines Limited (REL) and the French Aerospace Lab (ONERA) have a common interest in researching future space launch architectures and technologies, including the impact of using air-breathing propulsion systems. The primary objective of this joint study is to assess and quantify the potential advantages and benefits of air-breathing propulsion technology developed by REL named SABRE (Synergetic Air-Breathing Rocket Engine) for future European launch architectures. In that purpose, a conceptual study of two alternative Two-Stage-To-Orbit (TSTO) vehicles is carried out using the SABRE engine for the first stage[18] and a LOx/CH4 rocket engine for the second stage.[22]

Launch vehicle reusability has the potential to lower the cost of access to space and significantly to increase the efficiency of space transportation. Reusable first stages combined with expendable upper stages are a promising first step towards fully reusable launch vehicles. Whether an air-breathing Reusable Launch Vehicle (RLV) could come to be accomplished mainly depends on the developments and research progresses of air-breathing combined engines. Various air-breathing combined cycles have been proposed.[9,14,27,41] REL has conducted lots of fundamental and key technology studies around SABRE engine.[18] SABRE engine presents the interest of being able to fly up to around 25km and Mach number 5.0 in air-breathing mode, limiting the need for liquid oxidizer during the atmospheric flight. Moreover, it combines air-breathing and rocket cycles into a single engine, removing the need to have two separated propulsion systems depending on the trajectory phase.

The goal of the present study is to analyze and compare two reusable launch vehicle concepts in terms of both feasibility, reusability and payload performance using SABRE technologies. The study is on-going and the presented results are preliminary. More analyses involving economical aspects, operational conditions and a development roadmap are under assessment.

Different past studies have focused on the use of SABRE engines,[17,25,43] or alternative Rocket-Based Combined Cycle engines[44,45] for TSTO vehicles. These studies differ by vehicle layouts, target mission, trajectory envelop and integration of the second stage.

DOI: 10.13009/EUCASS2019-454

For the two studied concepts, this paper presents the design assumptions, simulation tools, vehicle characteristics and configurations, and reference trajectories. The paper is organized as follows. In Section 2, the mission specifications and design assumptions are introduced. In Section 3, the design method and the different modeling tools are detailed for the propulsion, the aerodynamics, the geometry and sizing, the mass budget and the trajectory simulation. Then, in Section 4, the preliminary design and trajectory results are presented for the two concepts and a first comparison of the two configurations is presented in Section 5. In Section 6, preliminary results on Return To Launch Site (RTLS) are described. Finally, in Section 8, the on-going works around this project are presented and the future works are detailed.

2. Mission specifications and design assumptions

The present study focuses on TSTO vehicles with the first stage being reusable and the second stage expendable. The considered reference mission for the reusable TSTO vehicle is to inject a payload of 15t into LEO at 400km on a circular equatorial orbit. It corresponds to a reference mission, but flexibility in terms of payload mass and target orbit is sought.

The architecture configurations for reusable TSTO vehicle are numerous, and this paper focuses on winged RVL. In order to identify promising architecture choices, a literature review[3–5,8,10,12,17,20,23,24,29,32,35–40,44,45] of proposed concepts and existing vehicles has been carried out (Figure 1). These concepts have been reviewed with respect to the possibility to perform the target mission and to integrate two key technologies: SABRE (for the first stage) and a low cost LOx/CH4 gas generator cycle rocket engine (for the second stage). Moreover, specific attention has been made on abort scenarios and consequences in terms of architecture choices.

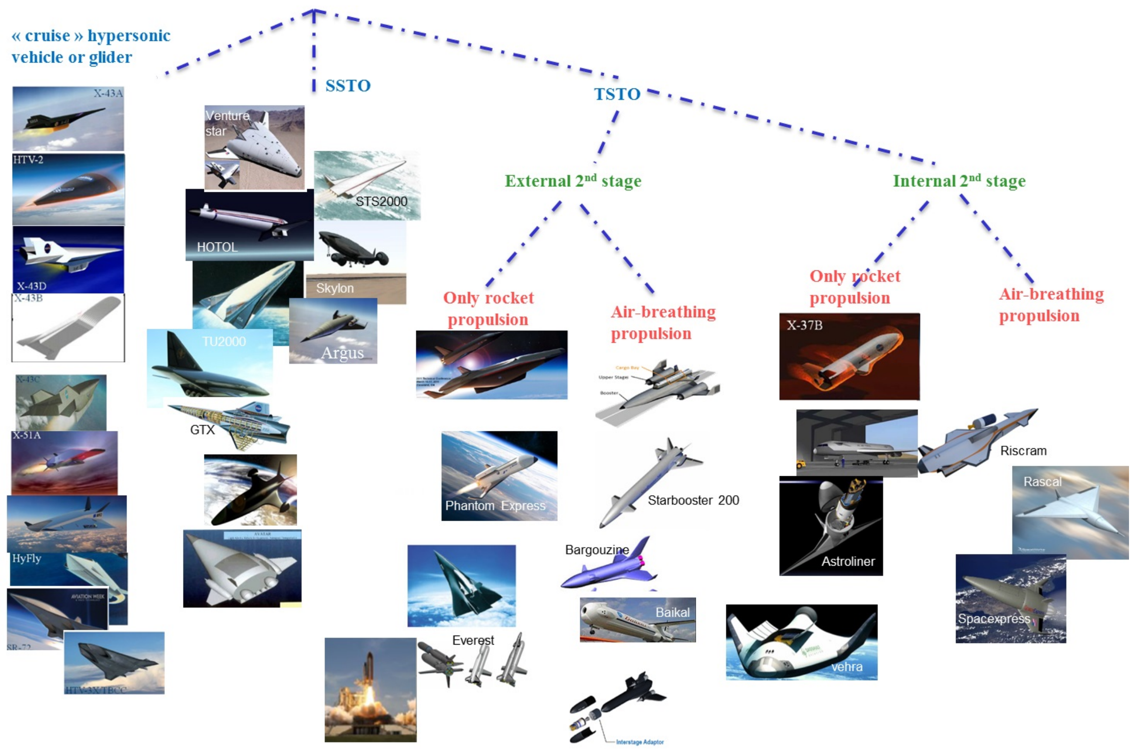

Figure 1: Literature review of the proposed winged RLV concepts

Following the literature review, two kinds of concepts may be suggested. As a reusable TSTO vehicle is designed using SABRE engines, high staging Mach number for the separation of the first and second stages is sought in order to minimize costs and efforts on the expandable second stage and to maximize the benefits from the reusable first stage.. The design of these concepts should be driven by a number of considerations such as the possibility (and types) of abort missions, the aerodynamics efficiency, the controllability as well as the thermal handling, due to the high Mach number at staging and the re-entry phase. The second stage is considered as expendable and its design is kept as simple as possible to minimize its cost using a low cost LOx/CH4 gas generator cycle rocket engine. Concerning the operational conditions in terms of abort, different criteria may be considered. The first criterion is relative to the

DOI: 10.13009/EUCASS2019-454

identification of the different possible failures. In the concepts under study, the main identified sources of failure seem to be relative to the propulsion system (in air-breathing or rocket modes). It is necessary to identify the nature of the failure and its time of occurrence during the mission in order to define a set of abort scenarios and their aftermaths on the vehicle architectures. For these different abort scenarios, the second criterion that has to be considered is the part of the launch vehicle that should be recovered. Indeed, the question of recovering only the first stage or the payload and / or the second stage is crucial in terms of the architecture choices for the considered mission. Finally, the location of the landing site (near the launch site or a distant site requiring a large cross-range capability) is a key-driver to the architecture choice. Depending on the failure and its time of occurrence, different options can be considered: either maximizing the use of aerodynamics forces, or using the air-breathing capability (or even the rocket capability if possible and air-breathing is in failure mode), to land either at a distant site or near the launch site. Based on these considerations, two kinds of architectures may be suggested and are briefly described in the following.

2.1 Payload-bay configuration

This concept consists of a winged first stage with the second stage (and payload) located in a payload bay inside the first stage. This architecture shares similarities with the SKYLON[19] but some differences in terms of geometrical shape are introduced (left of Figure 7). This architecture allows to enhance the aerodynamics efficiency (see Section 3.2), to set the location of the second stage such as the discrepancy of the center of gravity (CoG) locations before and after the stage separation is reduced, to ease the search of a trimmed configuration for both ascent and RTLS as the aerodynamics configuration and the CoG location is similar for both phases and to avoid the need of fairing for the second stage. Nevertheless, this concept requires integrating the second stage inside a payload bay, even if it is relatively small due to the high Mach number at staging and the use of Lox/CH4 propellant for the second stage. Adding bay doors to the vehicle increases the structural and the separation maneuver complexities. Moreover the internal volume required to accommodate the second stage leads to a large first stage which may be more expensive to acquire and more complex to design and operate. In terms of abort scenarios, having the second stage inside the first one may make more complex abort mission strategies (difficulty to jettison the elements inside the main stage in some cases of abort mission at high dynamic pressure involving the recovery of only the first stage). A consequence is for the first stage to be designed to land carrying the upper stage and payload filled with propellants, thus generating specific risks to be mitigated during abort situations.

2.2 In-front configuration

To avoid the complexity which stems from the presence of the payload bay and the abort capabilities, an alternative configuration could be to have a tube and wing architecture and integrate the second stage in front of the first stage as conventional expandable launchers (right of Figure 7). This configuration presents advantages to separate the second stage in a similar fashion as classical launch vehicles, to avoid the need for a payload bay (benefit in terms of structural complexity, avoid specific mechanisms for the second stage jettisoning), to reduce the volume of the first stage (no need to store the second and payload inside the first stage), to allow the possibility to jettison the upper stage and payload in case of abort mission, in order to safely recover the first stage that is the most expensive part of the launch vehicle.

This concept requires additional fairing for the second stage, resulting in additional mass that is not recovered. Moreover, the centering possibilities and controllability (for both ascent and return phases) are key-aspects due to the fact that the aerodynamic configuration differ significantly between ascent with payload in front and descent without.

For the presented results in the following, the study focuses on a vehicle that takes-off from Kourou and RTLS is the prefered recovery option (that will be studied in the future works as explained in Section 6).

3. Design method and modeling tools

3.1 Propulsion

The SABRE engine (Figure 2) is able to fly to over Mach 5 and an altitude of around 25 km in air-breathing mode. This allows to reduce the propellant consumption compared to the use of traditional full rocket engine in the atmospheric phases of the trajectory.

A simplified view of the SABRE engine cycle is represented in Figure 3.[18] It uses sub-cooled liquid hydrogen as fuel and sub-cooled liquid oxygen as the oxidizer in rocket mode. In the rocket mode, the engine operates as a closed cycle rocket engine. In the air-breathing mode, the liquid oxygen flow is replaced by the atmospheric air. The airflow

DOI: 10.13009/EUCASS2019-454

goes into the engine via an intake and is cooled by a pre-cooler heat exchanger. This latter is part of a closed cycle helium loop using the hydrogen fuel as the heat sink before it enters the combustion chamber. After cooling the air is compressed and fed to the combustion chamber.[18]

For the propulsion performance simulation, the present study is based on a SABRE engine deck, built by REL, that provides engine performances as a function of key parameters. Normalized specific impulse (Isp), gross thrust and fuel mass flow rates as a function of altitude and Mach number are illustrated in Figures 4, 5 and 6.

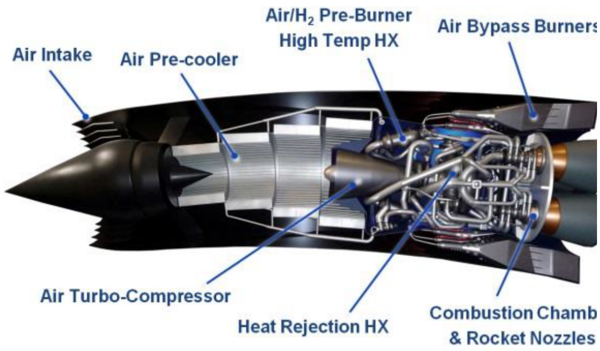

Figure 2: SABRE engine architecture[18]

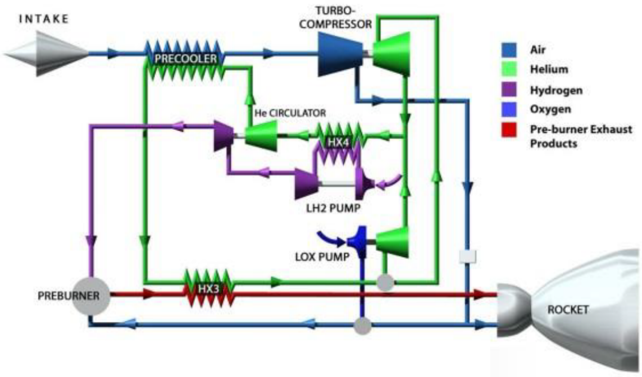

Figure 3: SABRE engine simplified cycle[18]

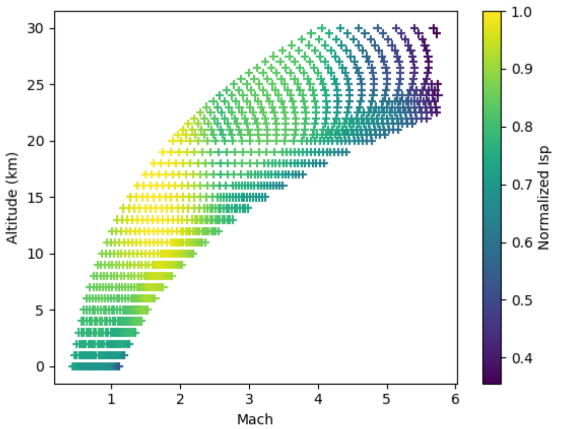

Figure 4: Illustration of the normalized Isp provided by the SABRE simulation deck as a function of Mach and altitude in air-breathing mode

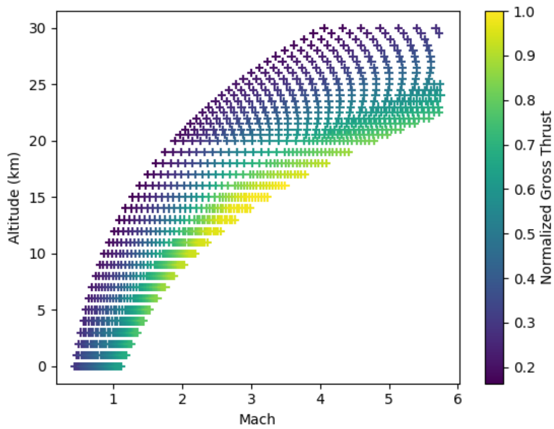

Figure 5: Illustration of the normalized gross thrust provided by the SABRE simulation deck as a function of Mach and altitude in air-breathing mode

The engine deck used for the study represents the best estimate of the SABRE installed nacelle performance available at the start of the current project. This engine deck was used as the basis for the SKYLON System SRR, performed by ESA in 2016. The toolset used was extensively reviewed by ESA experts as part of this process. Although validation data must await results from REL ongoing experimental programmes (HTX, DEMO-A, DEMO-N)[42],[33] at present it is believed that the model represents a good level of performance fidelity for the installed nacelle systems, suitable for preliminary systems studies such as that reported here.

The deck is based on Equivalent AirSpeed (EAS) and altitude as independent variables. The nacelle flow rates (air and fuel), gross thrust, and drag terms (momentum, spillage, external and base drags) are provided as dependent variables. System performance is calculated via an REL code which solves generalised, multiple, coupled networks of fluid paths, each containing an arbitrary number of components. All physical components within the engine (heat exchangers, turbomachinery, combustion zones and intakes and nozzles) are modeled based on physically dimensioned models and include reasonable loss/efficiency assumptions, although some simplifications are used for ducting and other connecting components. The deck supplied is generated using perfect gas models for all core flows, and a semi-perfect gas assumption within the combustion zones. Enthalpy is conserved at system and subsystem boundaries. More

DOI: 10.13009/EUCASS2019-454

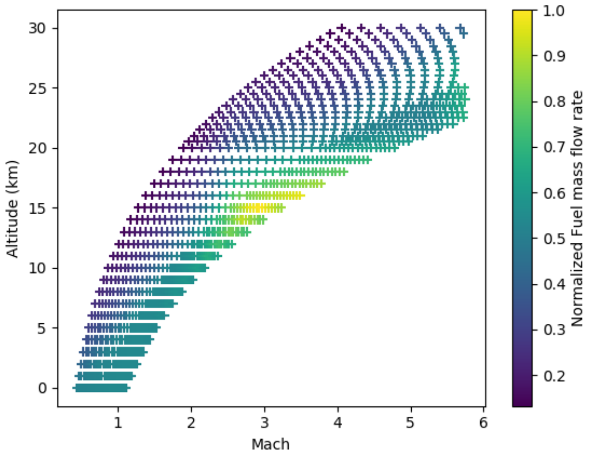

Figure 6: Illustration of the normalized fuel mass flow rate provided by the SABRE simulation deck as a function of Mach and altitude in air-breathing mode

Table 1: Second stage main propulsive characteristics using CNES in house tools for preliminary dimensioning of cryogenic engine

Thrust (vaccum)	150kN
Engine cycle	Gas generator
Specific impulse	365s (upper stage)
Mass target	< 350kg
Fuel	Ch4 (methane)
Oxidizer	LOx (oxygen)
Engine overall length	< 3m

recent models now include complete real gas flow solutions, but these are not available at the start of this study.

Currently, the engine deck does not include the effect of incidence or sideslip on intake performance, and hence is not suitable for modelling high incidence flight. External and spillage drag estimates are provided by numerical simulation of the nacelle intake system, validated by ongoing experiments performed by Gas Dynamics and Bayern Chemie.[2]

The ascent trajectory typically assumes the engine to be operating at maximum throttle throughout the ascent. For return to base and/or abort analysis, the ability to throttle the engine in some manner is key. The SABRE engine is more complex than a conventional turbojet or turbofan, and hence multiple throttling strategies are possible. That most often used within REL assumes the use of a simple choke on the core flow path, which in effect biases the flow towards the ramjet and away from the core engine, while maintaining full capture. As the specific thrust of the ramjet is lower, this reduces the thrust, and as the fuel flow rate in the nacelle is dominated by the flow through the core, reduces fuel flows and potentially increases Isp. An engine deck with throttle capability was generated for this project, although it uses a lower fidelity tool with much simplified core flow model. This deck has been validated at the 100% throttle point by comparison with the ascent deck defined above, and found to produce errors in fuel burn over the entire ascent of less than 1% (admittedly errors for just the air-breathing segment are higher).

For the second stage, a low cost LOx/CH4 gas generatoir cycle rocket engine is used to scale the engine with the mission requirements. This engine[21,22] is a methane-oxygen propelled engine, which is interesting in terms of compactness for the second stage compared to hydrogen-oxygen engines. Its characteristics and performances are provided by CNES. So far, a 150 kN thrust is chosen for this second stage engine. This thrust is assumed to be close enough to an optimum regarding the first stage high velocity staging, and the 15t payload objective on LEO orbit. It uses a cycle comparable to the one that is studied in the Prometheus(c) program. It uses a gas genrator cycle, single shaft single turbine turbopump. It develops a 150 kN thrust with a targeted 365s specific impulse in vacuum conditions, and could benefit from throttling and versatility capacities. However, this engine cannot derive directly from the Prometheus since its thrust will keep one order of magnitude lower than the Prometheus's one. Therefore a

DOI: 10.13009/EUCASS2019-454

specific dimensionning work was conducted by CNES in order to define preliminary propulsive characteristics for this engine as shown in Table 1.

3.2 Geometry and sizing

Two configurations are studied for the reusable TSTO vehicle: a payload-bay configuration and an in-front configuration. These concepts differ by their integration of the second stage with respect to the first stage. In the payload-bay configuration, the second stage is integrated inside the first stage in the payload-bay located near the center of gravity (which evolves during the flight) while for the in-front configuration, the second stage is located in front of the first stage as in conventional launcher.

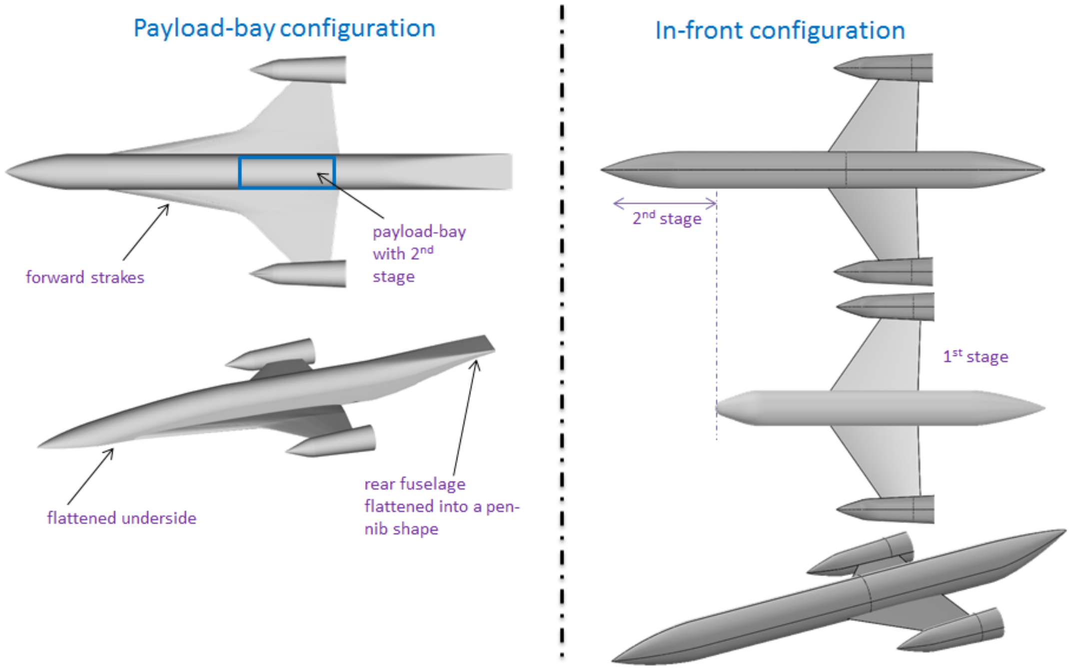

Figure 7: Illustration of the two first alternative configurations (payload-bay on the left and in-front on the right) represented without control surfaces

Moreover, to perform a sensitivity analysis with respect to the aerodynamical shape, two different shapes are analyzed. On the one side, the in-front configuration is a tube and wing concepts similar in shape to SKYLON.[18,19,30] For the in-front configuration, the main differences consist of the integration of the second stage that is not located in a payload-bay.

On the other side, the payload-bay concept presents an alternative aerodynamical shape. In order to improve thermal characteristics during reentry a flattened underside and elliptical nose is considered along with forward strakes to improve flight qualities and control as they provide forebody lift and nose-up pitching moment therefore canards are not required. In addition, the rear fuselage is flattened into a pen-nib shape in order to accommodate a flap for aero-control during high angle of attack reentry. Most of these aerodynamical improvements could be transfered to the in-front configuration, but in order to carry out a sensitivity analysis with respect to the aerodynamical shape (during ascent, re-entry, gliding phase, *etc.*) only the payload-bay configuration is considered with these geometrical characteristics.

In terms of tools to design the in-front and payload bay configurations, the geometry and sizing disciplines is a chain from geometrical modeler, to a parametric definition of the vehicle up to mesh generation for the aerodynamics discipline (Figure 8). Two geometrical modelers (OpenVSP[28] and FreeCAD[13]) have been used to create a parametric model for the vehicle configurations. This step consists in building a parametric model of the vehicle by defining sizing variables (*e.g.*, diameter, vehicle length, wing surface, wing root chord) that may be affected during the design process. By modifying such variables, it enables to reconstruct a coherent vehicle when some dimensions are changed.

Once the sizing variables have been modified and the geometrical model rebuilt, data and geometrical mesh may be generated for the aerodynamics discipline (*e.g.* CFD meshes). This entire chain of geometry and sizing is then

DOI: 10.13009/EUCASS2019-454

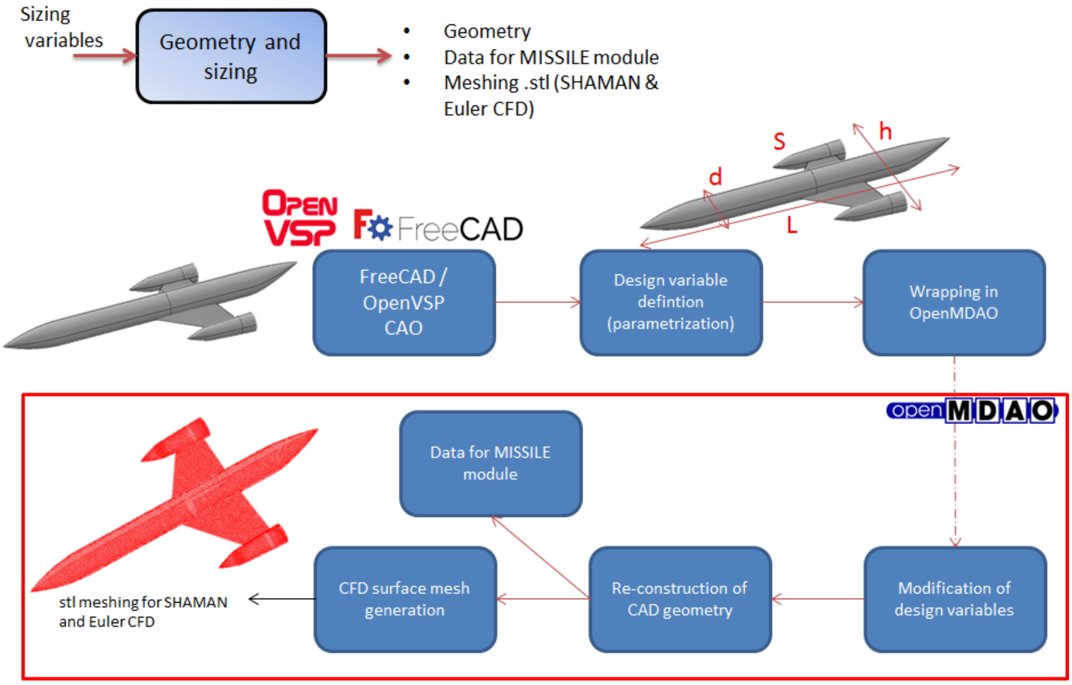

Figure 8: Geometry and sizing discipline integration from OpenVSP/FreeCAD to meshing generation for aerodynamics discipline

wrapped into OpenMDAO[15] as a component in order to have the possibility to define some of the sizing variables as design variables to enable a control by an optimization process.

3.3 Aerodynamics

The estimation of the aerodynamics of such launch vehicles is challenging. Indeed, the vehicles face hot reentry, resulting in a need to estimate its aerodynamics performance for high angles of attack (inducing separation flow, complex leeside flow, *etc.*), in a broad Mach number range : from a "standstill" to hypersonic speeds and in a trans-atmospheric flight path, from a continuum to a rarefied regime. In addition, the base drag in the non-propelled flight has be accounted especially at low speed. As the project is focused on the conceptual design phase, a multi-fidelity approach has been used in order to combine data from preliminary tools (SHAMAN and MISSILE[11]) with some Euler CFD calculations.[31]

SHAMAN is an engineering-level code which applies a combination of well-proven Local Surface Inclination (LSI) methods on an unstructured surface grid to compute the aerodynamics coefficients.

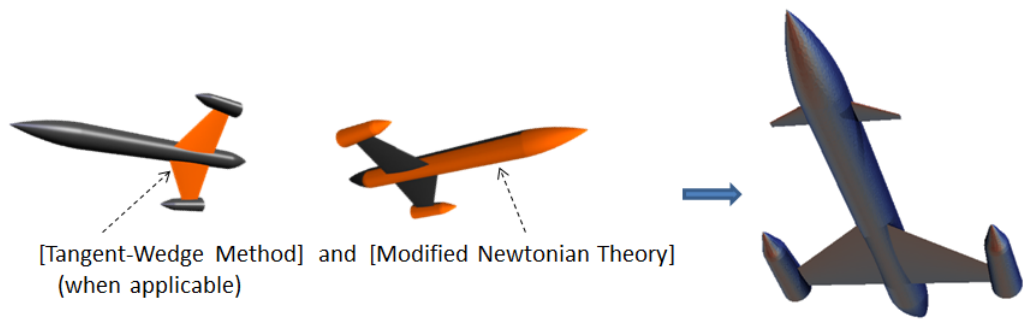

Figure 9: SHAMAN principle

To improve the accuracy of the aerodynamics estimation provided by the LSI methods, a limited number of Euler

DOI: 10.13009/EUCASS2019-454

CFD calculations (Figure 11) are used to anchor the engineering level estimates obtained using SHAMAN. However, even though the Euler CFD calculation should, in theory, predict both C_L and C_m satisfactorily well, the absence of shear stress under predicts C_D.

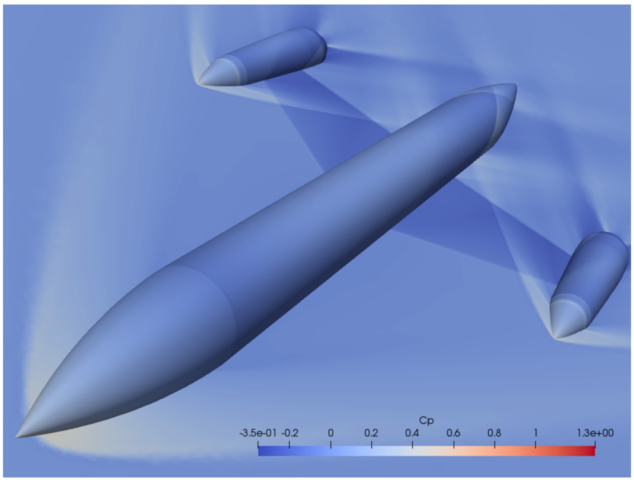

Figure 10: Example of CFD Euler calculation

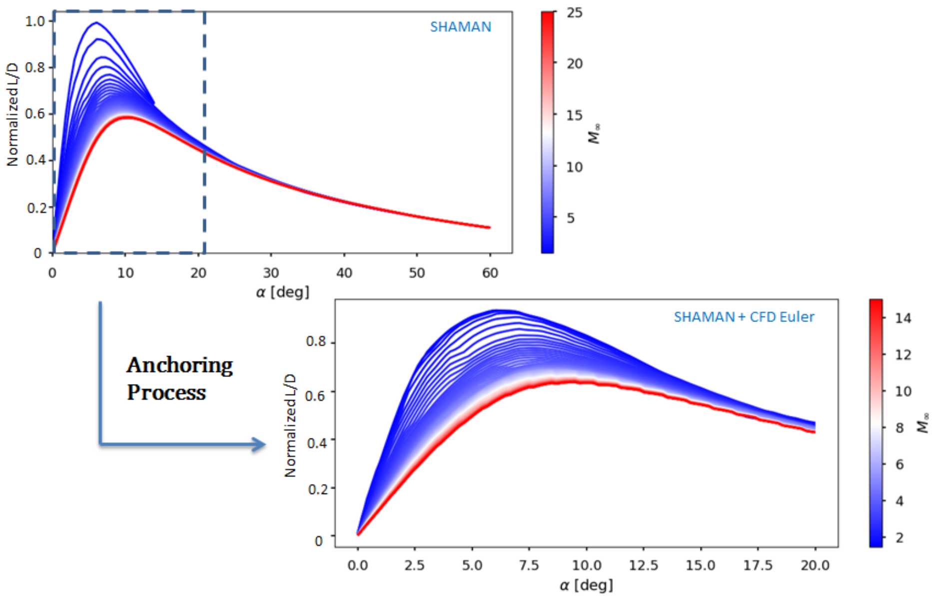

Figure 11: Example of normalized lift-to-drag improvements combining SHAMAN and Euler CFD as a function of angle of attack and Mach number.

Whenever the vehicle is not propelled (*e.g.*, part of its reentry or for some abort scenarios), a base drag term needs to be added relying on an empirical correlation of $C_{p,b}$ as a function of M_∞. This term can take up a significant part of the total drag especially at subsonic and low supersonic speed. Other empirical relations were used to account for the effect of shear stress (parasite drag) on the full drag coefficient estimates: laminar and turbulent flat plate relations applied to all wetted-area of the vehicle.

3.4 Mass budget

The mass budget discipline is in charge to estimate the inert mass of the vehicles including the primary structure (*e.g.*, tanks, wings, interstage) and the secondary masses (landing gears, avionics, power, *etc.*). Estimating the mass of such

DOI: 10.13009/EUCASS2019-454

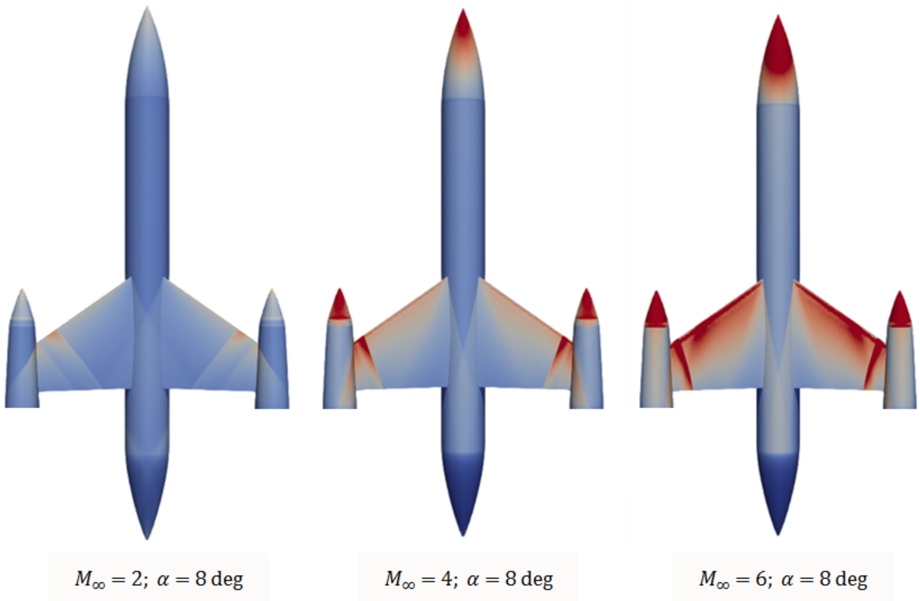

Figure 12: Example of Euler CFD calculations for different angles of attack and Mach numbers.

vehicles is challenging due to the absence of existing similar vehicle and the lack of data from past vehicles. For the conceptual design phase, Mass Estimating Relationships (MERs) have been used from the literature.[6,7,16,26,34] The mass budget estimation is decomposed according to the different components of the launch vehicles. Three main types of inputs are required for MERs: propulsion and geometry disciplinary outputs (diameters, lengths, surfaces and volumes of components, *etc.*), trajectory loads (*e.g.*, axial and lateral accelerations, dynamic pressure, heat flux) and technological choices (structural material, tanks type and layout, *etc.*). The implemented MERs are based on a comprehensive set collected from various sources.[6,7,16,26,34] The SABRE engine mass is provided by Reaction Engine Limited and the second stage rocket engine mass by CNES.

3.5 Trajectory simulation

The vehicles are modeled as a point mass in an Earth rotating frame with 3 degrees of freedom for all phases of the mission. The state vector contains seven variables for positions, velocities and the vehicle mass. The equations of motion are integrated using a 5 order Runge-Kutta technique. The vehicle control variables are the throttling of the engine, the pitch angle and the bank angle of the vehicle. The propulsion system is non - gimbled, the thrust vector produced is aligned with the longitudinal body axis of the vehicle. In order to define the optimal trajectory with the optimal vehicle configuration, the trajectory control variables are defined as design variables in the multidisciplinary design optimization problem. Moreover, several constraints are added to ensure the satisfaction of the mission (*e.g.*, injection of the payload to the target orbit, return to the launch site) along with the satisfaction of the maximal allowed loads undertaken during the flight (axial and lateral loads, dynamic pressures, *etc.*).

The trajectory starts with an horizontal lift-off (not simulated, the trajectory is initialized at 50m of altitude and a Mach number of 0.5) and then an air-breathing flight powered by SABRE is considered. This phase lasts until around 25km and Mach number 5.0. At these conditions, the SABRE engine is switched to rocket mode and uses the liquid oxydizer stored in the first stage. Then, a more standard rocket phase is done until the propellant used for the ascent is burnt. Then, a short ballistic flight is carried out to increase the altitude in order to satisfy a jettison condition on the heat flux for the second stage. Then, the second stage is jettisoned and carries on with its rocket flight. Finally, a coasting phase is performed in order to reach the final orbit that is circularized. In the meantime, the first stage re-enters into the atmosphere and returns to launch site using powered SABRE engines in air-breathing mode.

3.6 Multidisciplinary Design Analysis and Optimization (MDAO)

In order to identify the optimal architectures and to carry out parametric analyses, the multidisciplinary simulation is done using OpenMDAO[15] to integrate the different disciplines and to perform launch vehicle design and trajectory

DOI: 10.13009/EUCASS2019-454

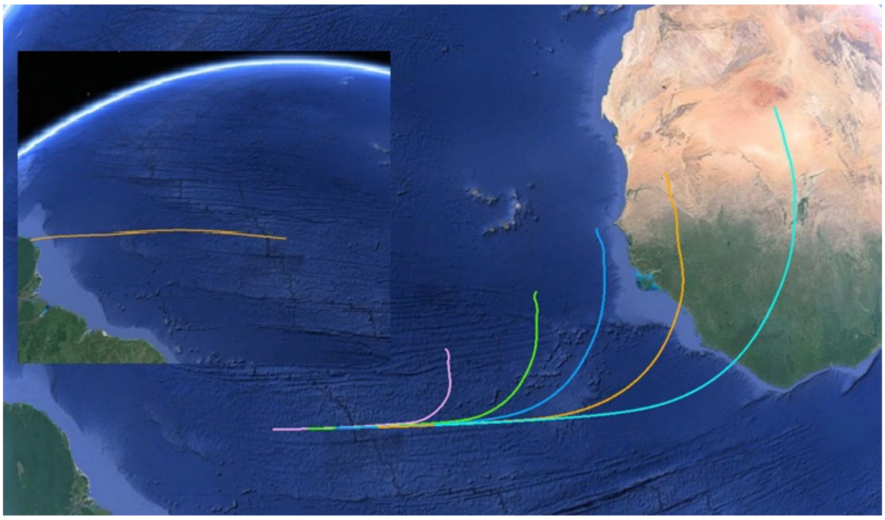

Figure 13: Example of trajectory simulations (ascent phase in left, and downrange re-entry in right).

optimization (Figure 14).

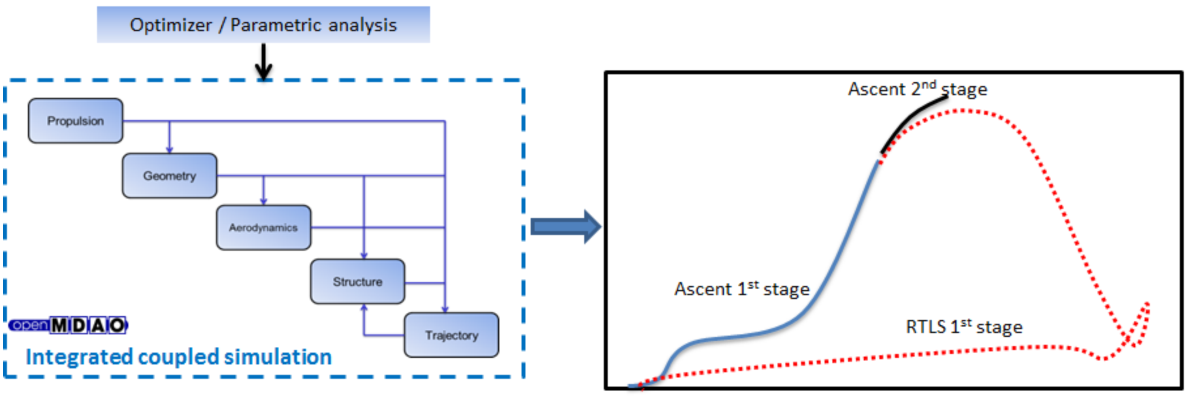

Figure 14: Integrated simulation multidisciplinary process.

This multidisciplinary approach allows to account for the interdisciplinary couplings in the design process to ensure the interdisciplinary feasibility.

4. Optimization results and discussions

In order to compare the two concepts, MDAO is carried out to optimize the launch vehicle trajectory and propellant masses needed for the mission. The optimization problem consists in minimizing the Gross Lift-Off Weight (GLOW) while ensuring the payload injection into the target orbit and the satisfaction of the maximal allowed loads. Different staging conditions between the first and the second stages are considered (velocity of 5500m/s, 6000m/s and 6500m/s) in order to evaluate its impact on the launch vehicle design. The results obtained with the payload-bay configuration are presented in Section 4.1 and the in-front configuration in Section 4.2.

The preliminary results presented in the following Sections do not account for the required propellants for the RTLS, only account the propellant masses for the ascent is considered. In future works, the analyses will account for these additional propellant masses (see Section 8 on the perspectives).

DOI: 10.13009/EUCASS2019-454

4.1 Payload-bay configuration

4.1.1 Ascent trajectories

The altitude, velocity and mass as functions of time for the three considered staging conditions are represented in Figures 15, 16 and 17. Considering these Figures, the different phases of the trajectory are distinguished: first an ascent phase up to 25km of altitude with a constant altitude phase allowing to increase the velocity up to Mach 5. Then, an increase of the altitude with a high rate corresponding to the switch from air-breathing to rocket modes for the SABRE engines as it can be seen in the mass flow rate. Following the rocket phase of the first stage, the SABRE engines are cut-off and a short ballistic flight is carried out to increase the altitude. Then the two stages are separated and the second stage engine is ignited until the start of the coasting phase (which is not represented on the Figures).

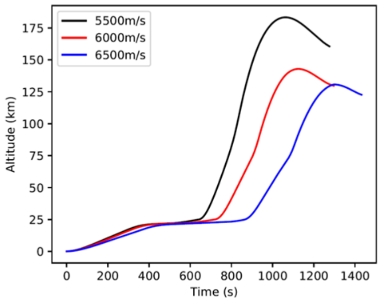

Figure 15: Altitude evolution for the ascent trajectory for the payload-bay configuration (without coasting phase)

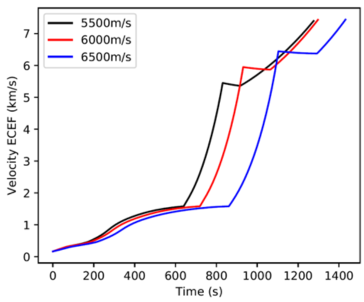

Figure 16: Velocity evolution for the ascent trajectory for the payload-bay configuration (without coasting phase)

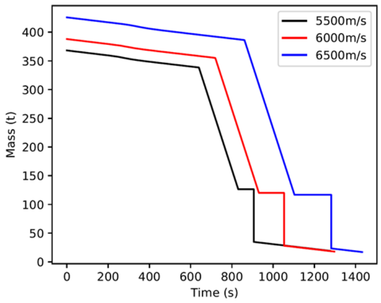

Figure 17: Mass evolution for the ascent trajectory for the payload-bay configuration (without coasting phase)

Table 2: GLOW and propellant masses for the payload-bay configuration depending on the staging conditions, AB: air-breathing mode and R: rocket mode

Staging condition (velocity)	**GLOW**	**Propellant mass 1st stage**	**Propellant mass 2nd stage**
5500 m/s	368t	242t (AB: 30t / R: 212t)	16t
6000 m/s	389t	268t (AB: 33t / R: 235t)	11t
6500 m/s	425t	308t (AB: 39t / R: 269t)	7t

Table 2 presents the GLOW and the distribution of the propellant masses between the first and second stages and between air-breathing and rocket mode for the SABRE engines. The GLOW increases with the Mach staging condition from 368t for 5500m/s to 425t for 6500m/s. It can be seen that the second stage uses a small amount of propellants, facilitating its integration in the payload-bay of the first stage especially with the high density of methane.

4.1.2 Gliding re-entry trajectories

In order to compare the aerodynamical shapes between the payload-bay and the in-front configurations, a gliding re-entry is performed considering two scenarios: maximization of the down-range and maximization of the cross-range. Moreover, these studies enable to illustrate the reachable footprint in case the SABRE engines do not re-ignite after atmospheric re-entry. The two problems consist in the maximization of the down-range and cross-range using the angle of attack and the bank angle as control variables. Figures 18, 19 and 20 present the re-entry with maximization of the down-range while Figures 21, 22 and 23 illustrate the cross-range maximization.

First, the different bumps on the altitude plots for the down-range and the cross-range maximizations are characteristics of classical skipping re-entry trajectories that use bounces on the atmosphere to increase the range covered. As expected, the higher the staging condition, the higher the down-range and cross-range reached by the vehicle during the re-entry.

Under certain conditions (in terms of maximal loads undertaken during the re-entry), in case of impossibility to re-ignite the SABRE engines, the preliminary analyses (Figure 24) show that it is possible to reach Cape Verde island or Ascension island to land the first stage which is an important aspect for abort scenarios.

DOI: 10.13009/EUCASS2019-454

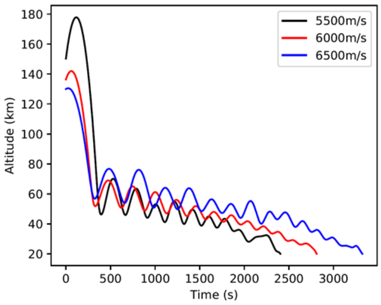

Figure 18: Altitude for the reentry trajectory for the payload-bay configuration, maximization of the down-range

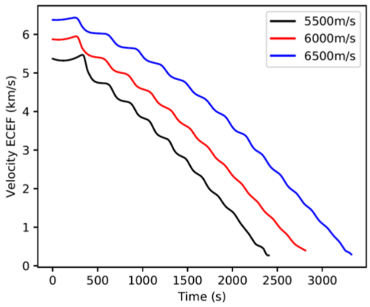

Figure 19: Velocity for the reentry trajectory for the payload-bay configuration, maximization of the down-range

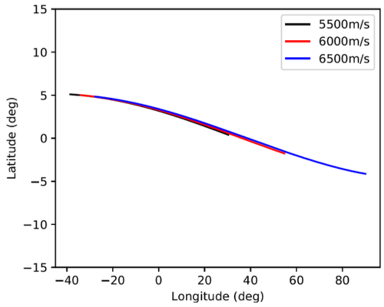

Figure 20: Longitude and latitude for the reentry trajectory for the payload-bay configuration, maximization of the down-range

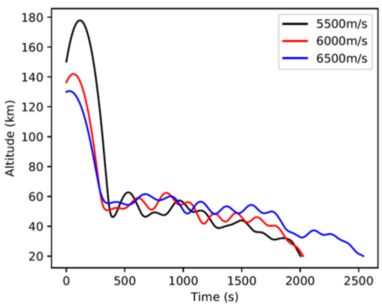

Figure 21: Altitude for the reentry trajectory for the payload-bay configuration, maximization of the cross-range

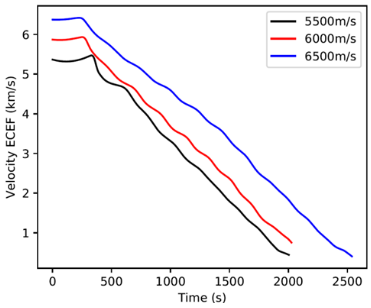

Figure 22: Velocity for the reentry trajectory for the payload-bay configuration, maximization of the cross-range

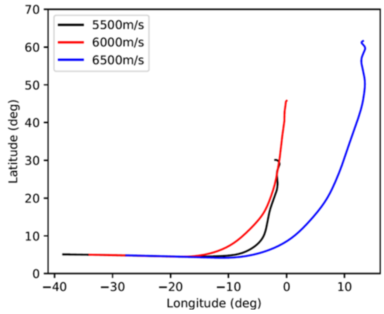

Figure 23: Longitude and latitude for the reentry trajectory for the payload-bay configuration, maximization of the cross-range

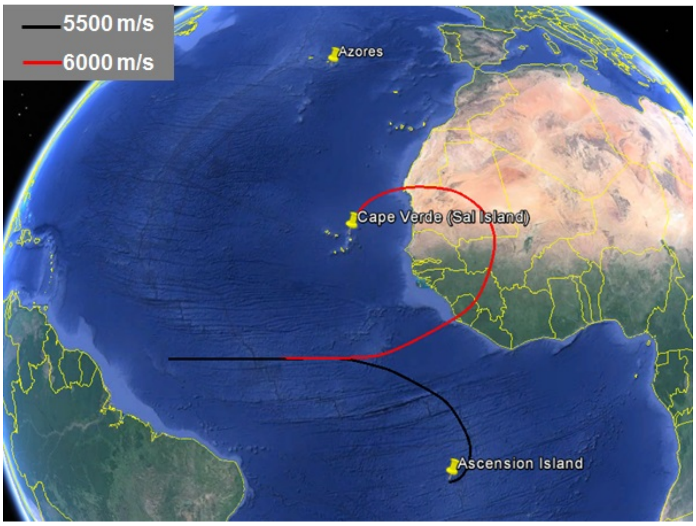

Figure 24: Possible landing sites depending on the staging velocity for the -bay concept for 5500m/s and 6000m/s.

4.2 In-front configuration

4.2.1 Ascent trajectories

Similarly to the analyses performed for the payload-bay configuration, ascent trajectory optimizations are carried out for the in-front configuration. The results are presented in Figures 25, 26 and 27. The results are closed to the payload-

DOI: 10.13009/EUCASS2019-454

bay ascent trajectories. The main differences lay into the vehicle mass due to the difference between the mass of the payload-bay and the need to integrate the second stage inside the first one, compared to a more conventional integration of the second stage in-front of the first one. These estimations are preliminary and more detailed analyses are required to confirm the first tendencies.

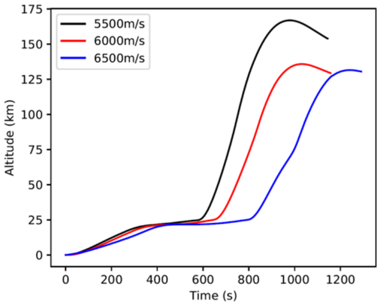

Figure 25: Altitude for the ascent trajectory for the in-front configuration

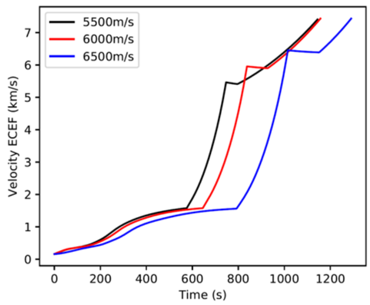

Figure 26: Velocity for the ascent trajectory for the in-front configuration

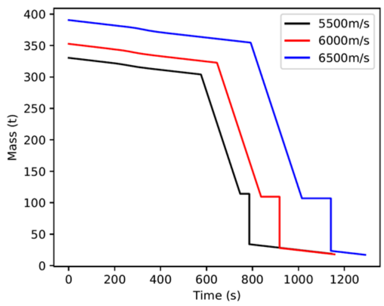

Figure 27: Mass for the ascent trajectory for the in-front configuration

Table 3 presents the GLOW and the distribution of the propellant masses between the first and second stages and between air-breathing and rocket mode for the SABRE engines. The GLOW increases with the Mach staging condition from 330t for 5500m/s to 391t for 6500m/s. The second stage is similar to the payload-bay configuration as the staging conditions are identical.

Table 3: GLOW and propellant masses for the in-front configuration depending on the staging conditions, AB: air-breathing mode and R: rocket mode

Staging condition (velocity)	**GLOW**	**Propellant mass 1st stage**	**Propellant mass 2nd stage**
5500m/s	330t	216t (AB: 26t / R: 190t)	16t
6000m/s	389t	243t (AB: 30t / R: 213t)	11t
6500m/s	391t	283t (AB: 36t / R: 247t)	7t

4.2.2 Gliding re-entry trajectories

The gliding performances of the in-front configuration are worst than the payload-bay concept and this is due to the aerodynamical shape improvements of this latter. The re-entry trajectories present the same skipping bumps as for the payload-bay concept.

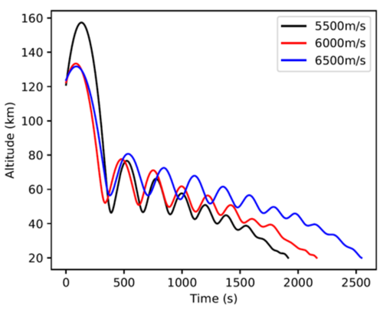

Figure 28: Altitude for the reentry trajectory for the in-front configuration, maximization of the down-range (without coasting phase)

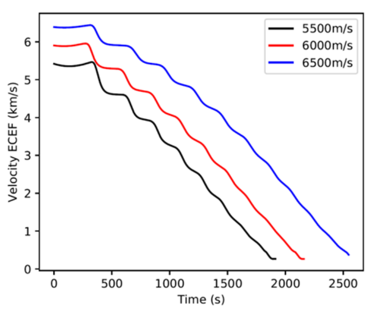

Figure 29: Velocity for the reentry trajectory for the in-front configuration, maximization of the down-range (without coasting phase)

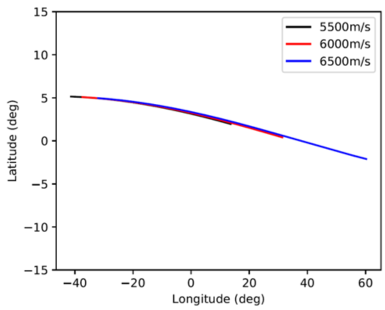

Figure 30: Longitude and latitude for the reentry trajectory for the in-front configuration, maximization of the down-range (without coasting phase)

Similarly to the payload-bay configuration, under certain conditions (in terms of maximal loads undertaken during the re-entry), in case of impossibility to re-ignite the SABRE engines, the preliminary analyses (Figure 24)

DOI: 10.13009/EUCASS2019-454

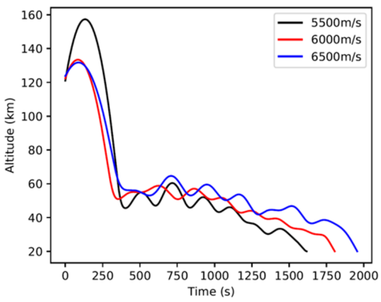

Figure 31: Altitude for the reentry trajectory for the in-front configuration, maximization of the cross-range

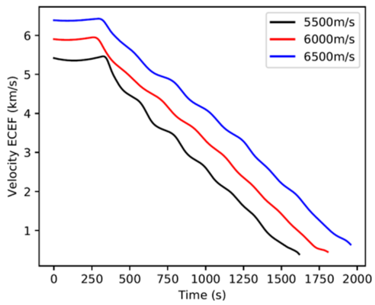

Figure 32: Velocity for the reentry trajectory for the in-front configuration, maximization of the cross-range

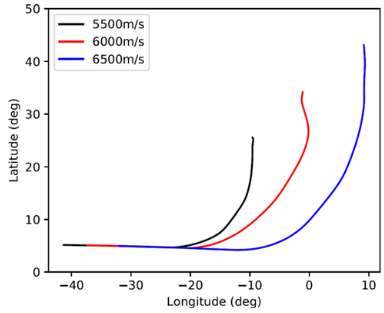

Figure 33: Longitude and latitude for the reentry trajectory for the in-front configuration, maximization of the cross-range

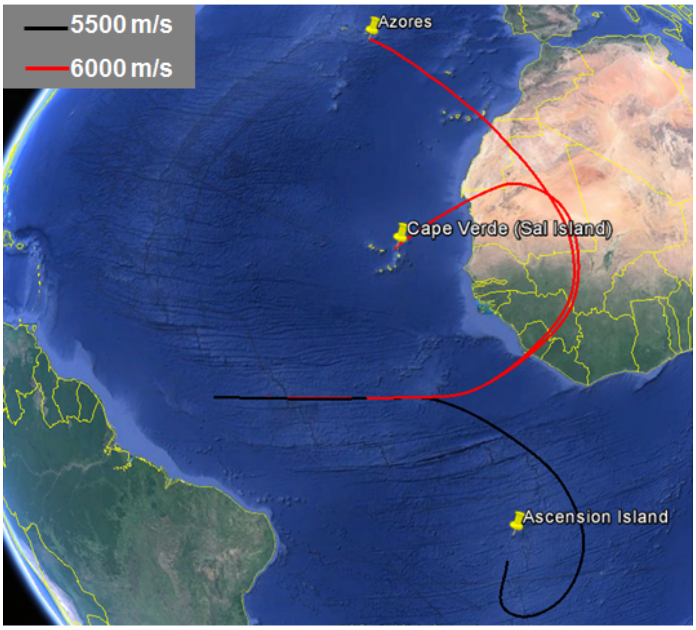

Figure 34: Possible landing sites depending on the staging velocity for 5500m/s and 6000m/s.

show that it is possible to reach Cape Verde island, Azores or Ascension island to land the first stage depending on the staging conditions.

5. Comparisons and analyses

From the preliminary analyses, the two configurations are able to inject a 15t payload into a 400km circular orbit taking-off from Kourou, without consideration of the return to launch site. The two configurations present similar results for the ascent trajectories, but some specificities differentiate them especially for the re-entry. Based on the current modeling fidelity, as presented in Figure 35, the payload-bay configuration tends to present a higher GLOW compared to the in-front for the same 2nd stage separation condition. However, the mass estimation needs to be refined in order to capture the mass differences with a higher fidelity (see future works). For the re-entry, for both the down-range and the cross-range maximizations in gliding mode (Figure 36), the payload-bay concept covers a higher range and this is due to the improvements in terms of aerodynamical shapes including the flattened underside, the forward stakes and the rear fuselage flattened into a pen-nib shape. Some of these improvements may be applied to the in-front configuration to improve its glider capabilities.

This improved gliding capabilities are interesting especially for the abort scenario in case the SABRE engines do not re-ignite during the re-entry. It offers the possibility to reach a distant landing site that is not Kourou (*e.g.*, Azores,

DOI: 10.13009/EUCASS2019-454

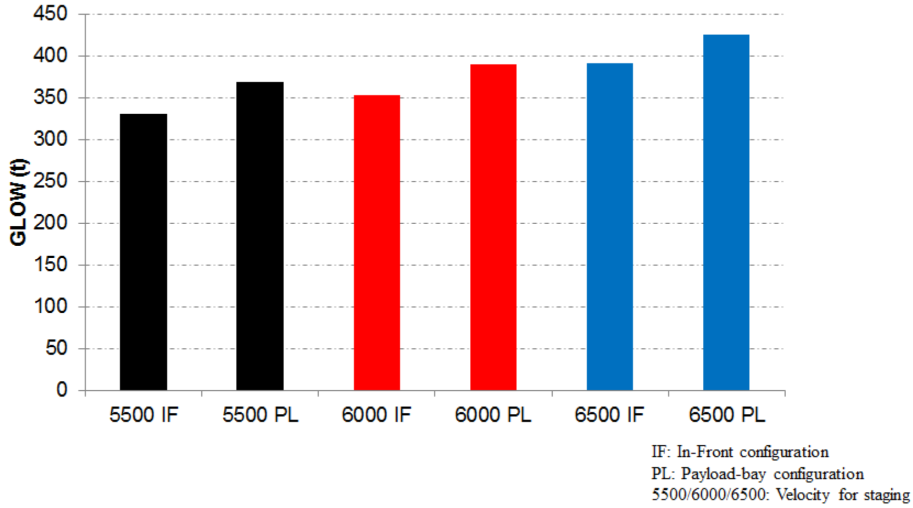

Figure 35: Comparison of the GLOW for the two concepts and the different staging conditions.

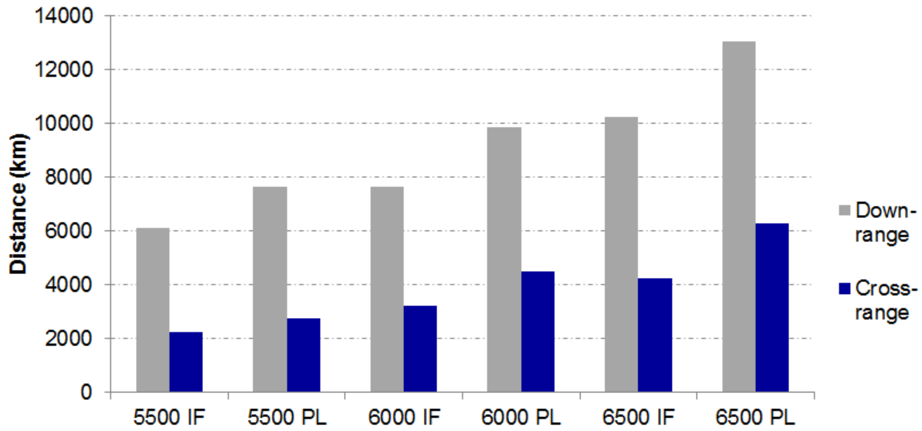

Figure 36: Comparison of the distance covered during gliding re-entry for the two concepts and the different staging conditions.

Cape Verde, Ascension island) where a runway of at least 3km is available.

6. Return to launch site

Simulations of powered RTLS using SABRE engine in air-breathing mode have been performed to provide a first estimate of the quantity of propellant needed to return to Kourou after the stage separation. After the 2nd stage separation, the first stage performs a high angle of attack re-entry into the atmosphere and then starts to carry out a u-turn. When the conditions for re-ignitition of the SABRE engines in air-breathing mode are reached (around 25km, Mach 5.0), a powered RTLS is performed (Figure 37). Further works on that aspect are currently under development.

DOI: 10.13009/EUCASS2019-454

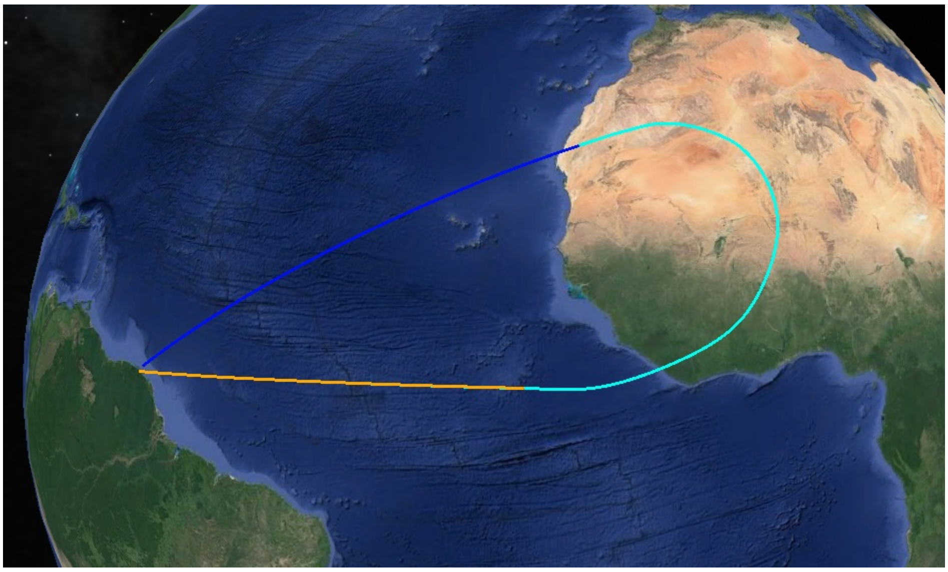

Figure 37: Illustration of return to launch site with a propelled air-breathing phase using SABRE engines. Orange trajectory corresponds to the ascent phase, then cyan trajectory is the ballistic phase, the re-entry and u-turn of the first stage while the blue trajectory corresponds to the air-breathing propelled phase to return to the launch site.

7. Study at Reaction Engines Limited

A parallel conceptual study is being conducted at REL using an independent toolset, whilst applying common top-level assumptions. This approach allows for direct comparison of the results and preliminary data has demonstrated a strong correlation between the two studies. The REL results will be published at a later date once the study has been concluded.

Moreover, a sensitivity to the second stage engine is under analysis, with a low cost LOx/CH4 gas generator cycle rocket engine of 180kN of thrust. This choice enables to compare in further analysis with a full LOX/LH2 TSTO system using the well known 180kN Vinci(c) engine that will propel Ariane 6 Upper Liquid Propulsive Module.[1]

8. Conclusions and perspectives

This paper presented an on-going study between CNES, REL, ONERA and UKSA on launch vehicle design of reusable TSTO vehicles integrating SABRE technologies. The present study focused on two TSTO vehicles to evaluate the potential interest of the combination of SABRE and a low cost LOx/CH4 gas generator cycle rocket engine on an integrated concept. Two alternative concepts are analyzed: a payload-bay configuration and an in-front configuration.

Under the current assumptions of SABRE and the low cost LOx/CH4 gas generator cycle rocket engine engine performances, at the conceptual design level, a TSTO vehicle seems to be a feasible option for the considered mission. The two studied concepts present important similarities but also specificities especially with respect to the second stage integration and their performances in gliding mode. Among the different analyses, a key aspect that is highlighted is the importance of aerodynamical shape design to gain important gliding capabilities in case of SABRE engine deficiencies during the re-entry. Different ascent trajectories considering various staging conditions have been presented for the two concepts along with some re-entry trajectories in gliding mode. Moreover, preliminary trajectory analyses showed the possibility to reach distant landing site in gliding mode under certain conditions. Some key influential parameters and intricate behaviors have been, analyzed, more particularly through a sensitivity to the stage separation conditions for the two concepts.

This on-going project has more analyses to perform including the full RTLS phase simulation and optimization but also some abort scenario simulations. It will also be necessary to study the controllability of such vehicle especially for the in-front concept due to the different vehicle configurations for the ascent and the re-entry (aerodynamical performances, evolution of the center of gravity, *etc.*). As a result, these preliminary analyses provide insight into technological requirements to achieve the target mission using advanced propulsion technologies. The objective of this project is to finalize a conceptual study of these vehicles including also recovery and refurbishment assessments, economical aspects, operational conditions as well as a preliminary development roadmap.

DOI: 10.13009/EUCASS2019-454

9. Acknowledgments

This project is part of an agreement between Centre National d'Etudes Spatiales (CNES), the UK Space Agency (UKSA) and Reaction Engines Limited (REL), this work is funded by CNES for the ONERA works.

References

[1] P Alliot, J-F Delange, V De Korver, J-M Sannino, A Lekeux, and B Vieille. Vinci®, the european reference for ariane 6 upper stage cryogenic propulsive system. *Progress in Propulsion Physics–Volume 11*, 11:481–494, 2019.

[2] James Barth, Cristoph Bauer, Richard Varvill, and Guido Kurth. Progress on the development and testing of the sabre air intake. In *3AF Space Propulsion Conference, May 2016*, 2016.

[3] Paul Bartolotta, Alan W Wilhite, Mark Schaffer, Randall T Voland, and Larry Huebner. Horizontal launch: A versatile concept for assured space access. *Report of the NASA-DARPA Horizontal Launch Study, NASA SP 2011-215994*, 2011.

[4] W Berry and H Grallert. Performance and technical feasibility comparison of reusable launch systems: A synthesis of the esa winged launcher studies. *Acta astronautica*, 38(4-8):333–347, 1996.

[5] Leonid Bussler and Martin Sippel. Comparison of return options for reusable first stages. In *21st AIAA International Space Planes and Hypersonics Technologies Conference*, page 2137, 2017.

[6] Francesco Castellini. Multidisciplinary design optimization for expendable launch vehicles. 2012.

[7] Jeff Cerro, Zoran Martinovic, Philip Su, and Lloyd Eldred. Structural weight estimation for launch vehicles. 2002.

[8] Sergio Chiesa, Gianpiero Russo, Marco Fioriti, and S Corpino. Status and perspectives of hypersonic systems and technologies with emphasis on the role of sub-orbital flight. *Aerotecnica Missili & Spazio*, 94(2):81–90, 2015.

[9] Russell Daines and Corin Segal. Combined rocket and airbreathing propulsion systems for space-launch applications. *Journal of Propulsion and Power*, 14(5):605–612, 1998.

[10] Julien de Mûelenaere and Juan J Alonso. High-fidelity trajectory based mdo for the conceptual design of an air-launched spaceplane. In *2018 AIAA/ASCE/AHS/ASC Structures, Structural Dynamics, and Materials Conference*, page 0416, 2018.

[11] P Denis. Onera's aerodynamic prediction code- missile. In *RTO/AGARD, Symposium on Missile Aerodynamics, Sorrento, Italy, May 11-14, 1998, ONERA, TP*, number 1998-56, 1998.

[12] Thino Eggers, Robert Dittrich, and Richard Varvill. Numerical analysis of the skylon spaceplane in hypersonic flow. In *17th AIAA International Space Planes and Hypersonic Systems and Technologies Conference*, page 2298, 2011.

[13] Brad Falck, Daniel Falck, and Brad Collette. *Freecad [How-To]*. Packt Publishing Ltd, 2012.

[14] Víctor Fernández Villacé. *Simulation, Design and Analysis of Air-Breathing Combined-Cycle Engines for High Speed Propulsion*. PhD thesis, Aeronauticos, 2013.

[15] Justin S. Gray, John T. Hwang, Joaquim R. R. A. Martins, Kenneth T. Moore, and Bret A. Naylor. OpenMDAO: An Open-Source Framework for Multidisciplinary Design, Analysis, and Optimization. *Structural and Multidisciplinary Optimization*, 59:1075–1104, 2019.

[16] Gary J Harloff and Brian M Berkowitz. Hasa: Hypersonic aerospace sizing analysis for the preliminary design of aerospace vehicles. 1988.

[17] Barry M Hellman, John E Bradford, Brad D St. Germain, and Kevin Feld. Two stage to orbit conceptual vehicle designs using the sabre engine. In *AIAA SPACE 2016*, page 5320. 2016.

[18] Mark Hempsell. Progress on the skylon and sabre. In *Proceedings of the International Astronautical Congress*, volume 11, pages 8427–8440, 2013.

DOI: 10.13009/EUCASS2019-454

[19] Mark Hempsell, Roger Longstaff, and A Bond. Skylon users manual. *Reaction Engines Limited*, 1, 2010.

[20] EH Hirschel and C Weiland. Design of hypersonic flight vehicles: some lessons from the past and future challenges. *CEAS Space Journal*, 1(1-4):3–22, 2011.

[21] A Iannetti, N Girard, D Tchou-Kien, C Bonhomme, N Ravier, and E Edeline. Prometheus, a lox/lch4 reusable rocket engine. In *7th European Conference for Aeronautics and Aerospace Sciences (EUCASS)*, 2017.

[22] Alessandra Iannetti, Nathalie Girard, Nicolas Ravier, Emmanuel Edeline, and David Tchou-Kien. Prometheus, a low cost lox/ch4 engine prototype. In *53rd AIAA/SAE/ASEE Joint Propulsion Conference*, page 4750, 2017.

[23] Alexander Kopp, Sven Stappert, David Mattsson, Kurt Olofsson, Erik Marklund, Guido Kurth, Erwin Mooij, and Evelyne Roorda. The aurora space launcher concept. *CEAS Space Journal*, 10(2):167–187, 2018.

[24] Ajay Kothari, John Livingston, Christopher Tarpley, Venkatraman Raghavan, Kevin Bowcutt, and Thomas Smith. Rocket based combined cycle hypersonic vehicle design for orbital access. In *17th AIAA International Space Planes and Hypersonic Systems and Technologies Conference*, page 2338, 2011.

[25] Roger Longstaff and Alan Bond. The skylon project. In *17th AIAA International Space Planes and Hypersonic Systems and Technologies Conference*, page 2244, 2011.

[26] IO Macconochie and PJ Klich. Techniques for the determination of mass properties of earth-to-orbit transportation systems. 1978.

[27] C McClinton, J Hunt, R Ricketts, Paul Reukauf, and C Peddie. Airbreathing hypersonic technology vision vehicles and development dreams. In *9th International Space Planes and Hypersonic Systems and Technologies Conference*, page 4978, 1999.

[28] Robert A McDonald. Interactive reconstruction of 3d models in the openvsp parametric geometry tool. In *53rd AIAA aerospace sciences meeting*, page 1014, 2015.

[29] Stuart McIntyre, Travis Fawcett, Thomas Dickinson, Michael West, Christie Alisa Maddock, Alessandro Mogavero, Lorenzo Ricciardi, Federico Toso, Konstantinos Kontis, Kin Hing Lo, et al. A commercially driven design approach to uk future small payload launch systems. In *14th Reinventing Space Conference*, 2016.

[30] Unmeel Mehta, Michael Aftosmis, Jeffrey Bowles, and Shishir Pandya. Skylon aerospace plane and its aerodynamics and plumes. *Journal of Spacecraft and Rockets*, 53(2):340–353, 2016.

[31] Francisco Palacios, Thomas D Economon, Aniket Aranake, Sean R Copeland, Amrita K Lonkar, Trent W Lukaczyk, David E Manosalvas, Kedar R Naik, Santiago Padron, Brendan Tracey, et al. Stanford university unstructured (su2): Analysis and design technology for turbulent flows. In *52nd Aerospace Sciences Meeting*, page 0243, 2014.

[32] R Palumbo, G Morani, M De Stefano Fumo, C Richiello, M Di Donato, F Corraro, and L Vecchione. Concept study of an atmospheric reentry using a winged unmanned space vehicle. In *18th AIAA/3AF International Space Planes and Hypersonic Systems and Technologies Conference*, page 5857, 2012.

[33] Russ Payne, Carrie Lambert, Richard Varvill, and James Barth. Sabre demo–a – key challenges for a ground demonstrator. In *3AF Space Propulsion Conference, Barcelona, 14–18th May 2018, Paper SP2018–503*, 2018.

[34] R Rohrschneider. Development of a mass estimating relationship database for launch vehicle conceptual design. *AE8900 Special Project, School of Aerospace Engineering, Georgia Institute of Technology*, 2002.

[35] Martin Sippel, Chiara Manfletti, Holger Burkhardt, and Thino Eggers. Technical development perspective of reusable booster stages. In *12th AIAA International Space Planes and Hypersonic Systems and Technologies*, page 7057. 2003.

[36] Martin Sippel, Sven Stappert, Leonid Bussler, and Etienne Dumont. Systematic assessment of reusable first-stage return options. In *Proceedings of the International Astronautical Congress, IAC*, number D2. 4.4, 2017.

[37] Yu Sumin, Ch Bonnal, S Kostromin, and N Panichkin. Project of ariane 5 lv family advancement by use of reusable fly-back boosters (named "bargouzine"). *Acta Astronautica*, 61(11-12):1043–1052, 2007.

DOI: 10.13009/EUCASS2019-454

[38] Yuriy Sumin, Sergey F Kostromin, Nikolai Panichkin, Yves Prel, Mikhail Osin, David Iranzo-Greus, and Marco Prampolini. Development of the rfbb "bargouzine" concept for ariane-5 evolution. *Acta Astronautica*, 65(7-8):943–948, 2009.

[39] David Sziroczak and Howard Smith. A review of design issues specific to hypersonic flight vehicles. *Progress in Aerospace Sciences*, 84:1–28, 2016.

[40] Ming Tang and Ramon Chase. The quest for a robust, responsive, reliable, efficient and low cost space access capability. In *16th AIAA/DLR/DGLR International Space Planes and Hypersonic Systems and Technologies Conference*, page 7417.

[41] David M Van Wie, Stephen M D'Alessio, and Michael E White. Hypersonic airbreathing propulsion. *Johns Hopkins APL technical digest*, 26(4):430–437, 2005.

[42] R. Varvill. Sabre technology development: Status and update. In *accepted for presentation at the 8th European Conference for Aeronautics and Aerospace Sciences (EUCASS) Madrid. EUCASS 2019–307*, 2019.

[43] Richard Varvill and Alan Bond. A comparison of propulsion concepts for ssto reusable launchers. *JOURNAL-BRITISH INTERPLANETARY SOCIETY*, 56(3/4):108–117, 2003.

[44] Jianxing Zhou, Hong Lu, Haocheng Zhang, Lingbo Zhao, Jingmin Chen, and Riheng Zheng. A preliminary research on a two-stage-to-orbit vehicle with airbreathing pre-cooled hypersonic engines. In *21st AIAA International Space Planes and Hypersonics Technologies Conference*, page 2343, 2017.

[45] Jianxing Zhou, Yuting Xiao, Kai Liu, and Wenxue She. Preliminary analysis for a two-stage-to-orbit reusable launch vehicle. In *20th AIAA International Space Planes and Hypersonic Systems and Technologies Conference*, page 3536, 2015.